H bonding might facilitate binding by ensuring that a critical intercationic distance is maintained which is complementary to the architecture of the anionic species. The possibility of anion binding, which is raised by the study of the solution conformation of the Orn residues, is currently under investigation.

Acknowledgment. This work was supported by Grant GM-22432 from the National Institute of General Medical Sciences, U.S. Public Health Service, by BRSG Grant RR07003 awarded by the Biomedical Research Support Program, Division of Research Resources, National Institutes of Health, and by National Research Award 1T32 GM-07616 from the National Institute of General Medical Sciences. NMR spectroscopy was performed on the Bruker WM-500 NMR spectrometer at the Southern California Regional NMR facility, which is supported by National Science Foundation Grant CHE-7916324.

Registry No. Me_6GrS, 83573-52-8; GrS, 113-73-5; Orn, 70-26-8.

Structural Characterizations of Salts of $HCr(CO)_5^-$ and $(\mu\text{-}H)_2BH_2Cr(CO)_4^-$ and Studies of Their Interconversions

Marcetta Y. Darensbourg,*[1a] Robert Bau,[1b] Melodye W. Marks,[1b] Robert R. Burch, Jr.,[1c] Joseph C. Deaton,[1c] and Sydney Slater[1c]

Contribution from the Departments of Chemistry, Tulane University, New Orleans, Louisiana 70118, and the University of Southern California, Los Angeles, California 90007.
Received February 11, 1982

Abstract: At 0 °C, BH_3 reacted with $HCr(CO)_5^-$ in THF to abstract hydride, presumably producing coordinatively unsaturated $Cr(CO)_5^0$, which immediately aggregated with remaining $HCr(CO)_5^-$ to yield the very stable $(\mu\text{-}H)[Cr_2(CO)_{10}]^-$. At room temperature two bridging hydride products were obtained. In addition to the binuclear bridging hydride, a second product, $(\mu\text{-}H)_2BH_2Cr(CO)_4^-$, resulted from CO loss either prior to or following Cr–H---BH_3 adduct formation. The borohydride complex could be reconverted to $HCr(CO)_5^-$ on addition of CO; however, $(\mu\text{-}H)[Cr_2(CO)_{10}]^-$ was also formed in the process. Salts of both title anions were characterized by solution spectroscopic probes as well as X-ray structural analysis. Crystals of $[Ph_4P][HCr(CO)_5]$ were found to belong to the tetragonal space group $P4/n$, with a = 13.234 (2) Å, b = 13.234 (2) Å, c = 7.472 (2) Å, and Z = 2. $R(F)$ = 3.9% for 1796 reflections with $I > 3\sigma(I)$. Deep red crystals of $[PPN][(\mu\text{-}H)_2BH_2Cr(CO)_4]$ belong to the triclinic space group $P\bar{1}$, with a = 11.708 (3) Å, b = 14.572 (6) Å, c = 11.454 (3) Å, α = 101.98 (3)°, β = 91.69 (2)°, γ = 77.34 (3)°, and Z = 2. $R(F)$ = 6.6% for 2880 reflections with $I > 3\sigma(I)$. Most notably, $HCr(CO)_5^-$ showed bending of the crystallographically identical equatorial CO groups toward the hydride ligand ($\angle(CO)_{ax}$–Cr–$(CO)_{eq}$ = 95.4 (1)°), as has been exhibited by all mononuclear hydridocarbonyl complexes whose structures are known. Analysis of the ν(CO) infrared spectrum indicated that this pseudooctahedral structure persisted in solution. The hydride ligand induced only a very small trans effect on the Cr–C bond length with $Cr\text{–}C_{trans}$ = 1.852 (4) Å and $Cr\text{–}C_{cis}$ = 1.865 (3) Å. The hydride ligand was located 1.66 (5) Å from Cr. In contrast the Cr–C bonds of $(\mu\text{-}H)_2BH_2Cr(CO)_4^-$ showed considerable asymmetry with $Cr\text{–}C_{eq}$(trans to H) = 1.81 (1) and 1.82 (1) Å and $Cr\text{–}C_{ax}$(cis to H) = 1.87 (1) and 1.85 (1) Å. In addition, the axial CO groups bend away from the $[(\mu\text{-}H)_2BCr]$ planar unit, $\angle(CO)_{ax}$–Cr–$(CO)_{ax}$ = 175.6 (4)°, whereas the equatorial CO groups expand into the space made available by the small requirement of the $(\mu\text{-}H)_2B$ bidentate ligand, $\angle(CO)_{eq}$–Cr–$(CO)_{eq}$ = 94.8 (4)°. Carbon-13 NMR spectroscopy showed the CO groups of $(\mu\text{-}H)_2BH_2Cr(CO)_4^-$ to be stereochemically rigid at +30 °C whereas ^1H NMR spectroscopy showed rapid interchange of bridging and terminal hydrogens, even at −80 °C.

Introduction

Recent progress in the syntheses of soluble salts of $HM(CO)_5^-$ (M = Cr, Mo, W)[2] has allowed for the development of the chemistry of these highly reactive metal carbonyl hydrides.[3] Although they were reported by Behrens et al., some 20 years ago,[4] these simple metal carbonyl hydrides were unavailable in soluble form for solution characterization and the molybdenum derivative was unknown. The synthetic advancements made lately were based on (1) circumventing reactions that are of an aggregative acid/base type, i.e., the interaction of the metal hydride with a transition-metal Lewis acid, $[M(CO)_5^0]$ (Scheme I), and (2) the successful utilization of hydride from an inexpensive light main-group metal hydride source (Scheme II). As also shown in Scheme II a competing reaction that involves CO loss may occur and is prominent for M = Mo.

Scheme I

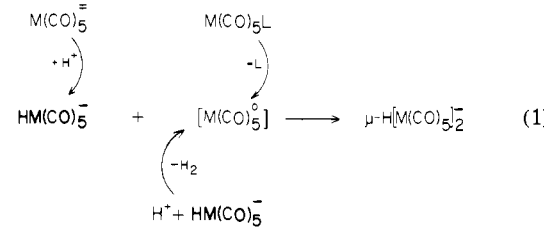

(1)

Scheme II

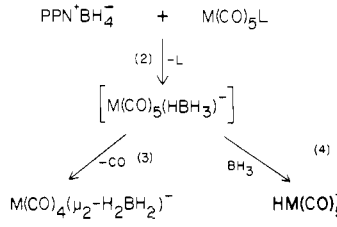

Concurrent developments that emphasized the need for understanding the chemical and spectral characteristics of $HM(CO)_5^-$ provided yet other routes to the hydrides.[3,5-7] The re-

(1) (a) To whom correspondence should be addressed at the Department of Chemistry, Texas A&M University, College Station, Texas 77843. (b) University of Southern California. (c) Tulane University.

(2) (a) Darensbourg, M. Y.; Slater, S. *J. Am. Chem. Soc.* **1981**, *103*, 5914. (b) Darensbourg, M. Y.; Deaton, J. C. *Inorg. Chem.* **1981**, *20*, 1644.

(3) Darensbourg, D. J.; Rokicki, A.; Darensbourg, M. Y. *J. Am. Chem. Soc.* **1981**, *103*, 3223.

(4) Behrens, H.; Weber, R. *Z. Anorg. Allg. Chem.* **1957**, *241*, 122. Behrens, H.; Vogl, J. *Ibid.* **1957**, *291*, 123. Behrens, H.; Vogl, J. *Chem. Ber.* **1963**, *96*, 2220.

0002-7863/82/1504-6961$01.25/0

Scheme III

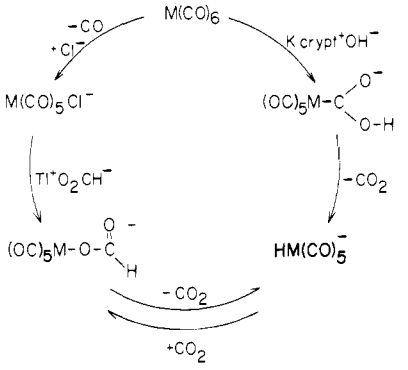

actions of Scheme III are of importance to the homogeneous catalysis of the water gas shift reaction by $M(CO)_6$ as well as to the activation of carbon dioxide by transition-metal hydrides. Although the mechanism of the CO_2 insertion into M–H bonds has not been completely delineated,[7] an acid/base interaction of the $M-H^{\delta-}\cdots{}^{\delta+}CO_2$ type is expected to be of significance. The dynamic chemistry presented below deals with a similar acid/base interaction, $M-H^{\delta-}\cdots{}^{\delta+}BH_3$, and a rearrangement that results in CO loss and a bidentate borohydride ligand.

The stereochemical activity (or possible lack thereof) of the small hydride ligand has been a subject of interest to physical organometallic chemists and structural chemists for many years.[8] As a major missing character in the cast of mononuclear metal carbonyl hydrides, $HCr(CO)_5^-$ (**1**) has been structurally characterized by us as its Ph_4P^+ salt and the analysis is reported herein. In addition, the $(\mu\text{-H})_2BH_2Cr(CO)_4^-$ anion as its bis(triphenylphosphine)nitrogen(1+) (PPN^+) salt has similarly been thoroughly analyzed.

Experimental Section

All syntheses and reactions were carried out under O_2-free conditions with use of a combination of glovebox (Ar atmosphere), Schlenk line (Ar or N_2), or high-vacuum-line techniques. Solvents were freshly distilled under N_2 from an appropriate drying and O_2-scavenging agent. Borane was purchased as the tetrahydrofuran (THF) adduct from Aldrich; its titer was checked by the gas evolution technique.[9] Bis(triphenylphosphine)nitrogen(1+) borohydride was prepared by the ion exchange of $Na^+BH_4^-$ and PPN^+Cl^- in THF.[10] Carbon monoxide gas (Matheson) was used as received. Carbon-13 labeled CO gas (93.3% ^{13}CO) was obtained from Prochem, B.O.C. Ltd., London.

Preparations. $Ph_4P^+HCr(CO)_5^-$. This hydride was synthesized and obtained free of other salts by the method reported earlier.[2b] Orange-gold crystals suitable for X-ray crystallographic analysis were obtained by diffusing hexane into a saturated THF solution inside a closed container.

$Na^+HCr(CO)_5^-$. The precursor, $Na_2Cr(CO)_5$, was obtained by the Na/naphth reduction of $Cr(CO)_5(NC_5H_{11})$ in THF as described previously for the tungsten analogue.[2a] No ion-exchange agent was added in the protonation step. The solvent was removed in vacuo, resulting in a red gum, which was subsequently redissolved in THF. Upon addition of hexane $Na^+HCr(CO)_5^-$ was obtained as a microcrystalline solid. The salt is thermally and photolytically (room light) unstable in solution and also (but less so) in the solid state. The yield was ca. 50%.

$PPN^+(\mu\text{-H})_2BH_2Cr(CO)_4^-$. The synthesis and isolation of crystalline $PPN^+(\mu\text{-H})_2BH_2Cr(CO)_4^-$ to be used for the structure determination were similar to those reported for the Mo analogue.[10] Thus 0.52 mmol of $PPN^+Cr(CO)_5I^-$ and 1.79 mmol of $PPN^+BH_4^-$ were reacted in 35 mL of refluxing THF for 12 h. Following filtration through a sintered-glass funnel the solvent volume was reduced to ca. 15 mL and 20 mL of Et_2O was added to precipitate PPN^+I^- and excess $PPN^+BH_4^-$, which was filtered off. The red oil that resulted on the addition of 30 mL of pentane was then allowed to stand undisturbed in the dark for 12 h, following which time the red crystals that had formed were collected; yield ca. 70%. Anal. Calcd for $PPN^+Cr(CO)_4BH_4^-$: C, 66.96; H, 4.74; O, 8.92; Cr, 7.25. Found (Mikroanalytisches Laboratorium, Bonn): C, 66.28; H, 4.69; O, 9.01; Cr, 6.86. In concentrated THF solution the following bands are observed in the B-H stretching region of the infrared spectrum: 2415 (sh), 2365 (m), 2210 cm^{-1}. The ν(CO) infrared vibrational modes are observed at 2011 (w), 1884 (s, br), and 1835 (m) cm^{-1}.

^{13}C-Enriched $(\mu\text{-H})_2BH_2Cr(CO)_4^-$. The PPN^+ salt of ^{13}C-enriched $Cr(CO)_4BH_4^-$ was prepared in a manner similar to that described above with ^{13}C-labeled $PPN^+Cr(CO)_5Br^-$ as starting material. Enrichment of the bromide was achieved by stirring a THF solution of $PPN^+Cr(CO)_5Br^-$ under a ^{13}CO (93%) atmosphere for 2 h at 22 °C. The solvent was removed in vacuo, and the residue was used in subsequent preparations. The level of enrichment was estimated by IR spectroscopy to be ca. 20%.

Reactions of $HCr(CO)_5^-$ and $(\mu\text{-H})_2BH_2Cr(CO)_4^-$. All reactions were run in Schlenk flasks or in the glovebox and monitored by IR spectroscopy. Identification of products was based on comparison of IR spectra with those of well-characterized compounds.

Infrared Spectral Measurements. The IR spectra were taken of THF solutions in matched, sealed 0.1-mm NaCl cells with use of the Perkin Elmer 283B infrared spectrophotometer which was calibrated below 2000 cm^{-1} on water vapor. Absorbance spectra for relative intensity measurements were taken on 0.050 and 0.0050 M solutions of $PPh_4^+HCr(CO)_5^-$, and the areas under the A_1^2 and A_1^1 bands measured by planimeter. The ratio $(\text{area}(A_1^2)/\text{area}(A_1^1))$ was found to be 0.00880.

Nuclear Magnetic Resonance. Proton NMR spectra were measured on CD_3CN or THF solutions with a Varian EM390, a JEOL FX90Q (University of New Orleans), or a Bruker 180 (University of California, Berkeley) instrument. Carbon-13 spectra were taken on a JEOL FX60 instrument. All instruments were equipped with variable-temperature capabilities.

X-ray Crystal Structure Analyses. $Ph_4P^+HCr(CO)_5^-$. Single crystals of $Ph_4P^+HCr(CO)_5^-$ as obtained above were sealed in thin-walled glass capillaries under nitrogen. Crystal, instrument, and final refinement parameters for the structure, which was carried out by Crystalytics Co., may be found in Table I.

Intensity measurements utilized graphite-monochromated Mo Kα radiation and the ω-scanning technique with a 4° takeoff angle and a normal-focus X-ray tube. A total of 3003 independent reflections having

Table I. Summary of Crystal Data and Details of Refinement for $[Ph_4P][HCr(CO)_5]$ and $[PPN][Cr(CO)_4BH_4]$

	$[Ph_4P]$-$[HCr(CO)_5]$	$[PPN]$-$[Cr(CO)_4BH_4]$
mol wt	532.4	717.5
temp of data collection, K	293 ± 1	298
cryst dimens, mm	0.85 (max), 0.58 (min)	0.18 × 0.30 × 0.35
space group	$P4/n$	$P\bar{1}$
molecules/unit cell	2	2
cell constants		
a, Å	13.234 (2)	11.708 (3)
b, Å	13.234 (2)	14.572 (6)
c, Å	7.472 (2)	11.454 (3)
α, deg	90.00	101.98 (3)
β, deg	90.00	91.69 (2)
γ, deg	90.00	77.34 (3)
cell vol, Å^3	1308.7 (4)	1864.8 (11)
calcd density, g cm^{-3}	1.35	1.28
abs coeff, μ, cm^{-1}	5.6	4.5
reflctns collected	3003	4684
unique reflctns	3003	4431
reflctns used in anal.[a]	1796	2880
parameters (n_v)	106	273
final agreement factors[b]		
$R(F)$	0.039	0.066
$R(wF)$	0.052	0.074
radiation	graphite-monochromated Mo Kα (λ = 0.710 73 Å)	
autodiffractometer	Syntex $P\bar{1}$	Syntex $P2_1$

[a] $I > 3\sigma(I)$. [b] $R(F) = \Sigma||F_o| - |F_c||/\Sigma F_o$; $R(wF) = [\Sigma w(|F_o| - |F_c|)^2/\Sigma wF_o^2]^{1/2}$.

(5) Darensbourg, D. J.; Rokicki, A. *ACS Symp. Ser.* **1981**, *No. 152*, 107.
(6) Darensbourg, D. J.; Darensbourg, M. Y.; Burch, R. R., Jr.; Froelich, J. A.; Incorvia, M. J. *Adv. Chem. Ser.* **1979**, *173*, 106.
(7) Darensbourg, D. J.; Rokicki, A. submitted for publication in *J. Am. Chem. Soc.*
(8) McNeill, E. A.; Scholer, F. R. *J. Am. Chem. Soc.* **1977**, *99*, 6243 and references therein.
(9) This procedure was described in: "Quantitative Analysis of Active Boron Hydrides", Aldrich Technical Information leaflet, Aug 1975.
(10) Kirtley, S. W.; Andrews, M. A.; Bau, R.; Grynkewich, G. W.; Marks, T. J.; Tipton, D. L.; Whittlesey, B. R. *J. Am. Chem. Soc.* **1977**, *99*, 7154.

$2\theta \leq 71°$ were measured in four shells. A scanning rate of 6.0°/min was employed for the scan between ω settings 0.50° respectively above and below the calculated Kα doublet value for those reflections having $3° < 2\theta_{Mo K\alpha} \leq 43°$, and a scanning rate of 4°/min was used for reflections having $43° < 2\theta_{Mo K\alpha} \leq 71°$. Each of these 1.00° scans was divided into 19 equal time intervals, and those 13 contiguous intervals that had the highest single accumulated count at their midpoint were used to calculate the net intensity from scanning. Background counts, each lasting for one-fourth the total time used for the net scan, were measured at ω settings 1.0° above and below the calculated value for each reflection. The six standard reflections, measured every 300 reflections as a monitor for possible disalignment and/or deterioration of the crystal, gave no indication of either. The intensities were corrected empirically for absorption effects with use of ψ scans for seven reflections having 2θ between 13 and 38°; the relative transmission factors ranged from 0.90 to 1.00. The intensities were then reduced to relative squared amplitudes, $|F_o|^2$, by means of standard Lorentz and polarization corrections.

Of the 3003 reflections examined, 1207 were eventually rejected as unobserved by applying the rejection criterion $I < 3.0\sigma(I)$, where $\sigma(I)$ is the standard deviation in the intensity computed from $\sigma^2(I) = (C_t + k^2B)$ where C_t is the total scan count, k is the ratio of scan time to background time, and B is the total background count.

The chromium atom was located from a Patterson synthesis; the remaining non-hydrogen atoms appeared in a single difference Fourier synthesis based on refinement parameters for the Cr atom ($R_1 = 0.534$ for 667 independent reflections having $2\theta_{Mo K\alpha} < 43°$ and $I > 3\sigma(I)$). Isotropic unit-weighted full-matrix least-squares refinement for the 12 non-hydrogen atoms gave R_1(unweighted, based on F) = 0.094 and R_2(weighted) = 0.093. Anisotropic refinement converged to $R_1 = 0.058$ and $R_2 = 0.065$ for 667 reflections.[11] These and all subsequent structure factor calculations employed recent tabulations of atomic form factors[12] and anomalous dispersion corrections for the scattering factors of the chromium and phosphorus atoms.[13]

All hydrogen atoms were located in a difference Fourier map calculated at this point. The final cycles of empirically weighted[14,15] full-matrix least-squares refinement, in which the structural parameters for all isotropic hydrogens and anisotropic non-hydrogen atoms were varied, converged to $R_1 = 0.039$, $R_2 = 0.052$, and GOF = 1.36[16] for 1796 independent reflections having $2\theta_{Mo K\alpha} \leq 71.0°$ and $I > 3\sigma(I)$. During the final cycle of refinement, no parameter (including those of hydrogen atoms) shifted by more than $0.04\sigma_p$ with the average shift being $<0.01\sigma_p$, where σ_p is the estimated standard deviation of the parameter. A final difference Fourier synthesis revealed no peaks present above 0.21 e/Å^3.

$PPN^+Cr(CO)_4BH_4^-$. Single crystals of $PPN^+Cr(CO)_4BH_4^-$ as obtained above were mounted in 0.3-mm glass capillary tubes under N_2 in the USC laboratories. Fifteen low-angle ($3° < 2\theta < 18°$) reflections were centered and were used in an autoindexing program. Three axial vectors were chosen to produce a triclinic cell, and the hkl values were assigned accordingly. The cell could not be reduced to one of higher symmetry. Fifteen higher angle ($15° < 2\theta < 25°$) reflections were then centered to obtain accurate cell constants and an orientation matrix. All crystal, instrument, and final refinement parameters are listed in Table I.

One hemisphere of data was collected by the $\theta/2\theta$ scan technique up to a 2θ limit of 45°. The crystal did not diffract much beyond that point. A variable-scan mode, from 3.5 to 16.0° min^{-1}, was employed with use of a scan width of 2.0°. Three check reflections were monitored every 75 reflections and showed no significant changes in the stability of the crystal or the diffractometer.

Table II

(A) Atomic Coordinates for Non-Hydrogen Atoms in Crystalline $[Ph_4P][HCr(CO)_5]$[a]

atom type[b]	fractional coordinates		
	x	y	z
Cr	0.2500[c]	0.2500[c]	−0.1631 (1)
P	0.7500[c]	0.2500[c]	0.0000[c]
O_1	0.2500[c]	0.2500[c]	0.2388 (4)
O_2	0.4213 (2)	0.1024 (2)	−0.2059 (4)
C_1	0.2500[c]	0.2500[c]	0.0847 (5)
C_2	0.3566 (2)	0.1589 (2)	−0.1867 (3)
C_{p_1}	0.6417 (1)	0.2537 (1)	0.1437 (2)
C_{p_2}	0.5680 (1)	0.3273 (2)	0.1270 (3)
C_{p_3}	0.4868 (2)	0.3275 (2)	0.2457 (4)
C_{p_4}	0.4799 (2)	0.2563 (2)	0.3787 (3)
C_{p_5}	0.5534 (2)	0.1835 (2)	0.3967 (3)
C_{p_6}	0.6347 (2)	0.1814 (2)	0.2801 (3)

(B) Atomic Coordinates for Hydrogen Atoms in Crystalline $[Ph_4P][HCr(CO)_5]$[a]

atom type	fractional coordinates			
	x	y	z	B, Å^2
H_{p_2}	0.575 (2)	0.378 (2)	0.044 (4)	4.6 (5)
H_{p_3}	0.435 (2)	0.377 (2)	0.239 (4)	6.2 (7)
H_{p_4}	0.423 (2)	0.254 (2)	0.456 (4)	5.5 (6)
H_{p_5}	0.547 (2)	0.132 (2)	0.483 (4)	6.2 (7)
H_{p_6}	0.687 (2)	0.128 (2)	0.291 (3)	4.6 (5)
H	0.250[c]	0.250[c]	−0.385 (7)	4.3 (10)

[a] The numbers in parentheses are the estimated standard deviations in the last significant digits. [b] Atoms are labeled in agreement with Figure 1. [c] This is a symmetry-required value and is listed without a standard deviation.

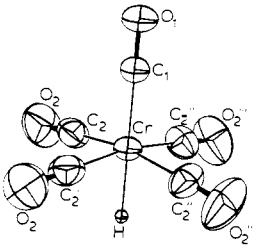

Figure 1. ORTEP plot of numbering scheme for the $HCr(CO)_5^-$ anion. Thermal ellipsoids show 50% probability.

The standard deviation of each intensity reading was estimated by using the expression[17]

$$\sigma(I) = [(\text{peak} + \text{background counts}) + [0.04(\text{net intensity})]^2]^{1/2} \quad (5)$$

The raw data were reduced to yield 2880 independent reflections satisfying the criterion $I > 3\sigma(I)$. The intensities were corrected for Lorentz, polarization, and absorption effects; transmission coefficients (normalized to unity) varied between 0.94 and 1.03.

The coordinates of the chromium atom were obtained from a Patterson map. The other non-hydrogen atoms were obtained from a series of difference-Fourier maps.[18] During least-squares refinement,[19] the parameters were blocked into two matrices: one with the scale factor, anion coordinates, and thermal parameters and the other with the cation coordinates and thermal parameters. The non-hydrogen atoms in the anion and the two phosphorus atoms were refined anisotropically while the other atoms were refined isotropically. After several cycles of least-squares refinement, the phenyl hydrogen atom positions were cal-

(11) The anisotropic thermal parameter is of the form $\exp[-0.25(B_{11}h^2a^{*2} + B_{22}k^2b^{*2} + B_{33}l^2c^{*2} + 2B_{12}hka^*b^* + 2B_{13}hla^*c^* + 2B_{23}klb^*c^*)]$.

(12) "International Tables for X-ray Crystallography"; Kynoch Press: Birmingham, England, 1974; Vol. IV, pp 149–150.

(13) Reference 12, pp 99–101.

(14) The weighting scheme used in the least-squares minimization of the function $\sum w(|F_o| - |F_c|)^2$ is defined as $w = 1/\sigma_F^2$.

(15) For empirical weights

$$\sigma_F = \sum_0^3 a_n|F_o|^n = a_0 + a_1|F_o| + a_2|F_o|^2 + a_3|F_o|^3$$

with the a_n being coefficients from the least-squares fitting of the curve

$$||F_o| - |F_c|| = \sum_0^3 a_n|F_o|^n$$

For $[Ph_4P][HCr(CO)_5]$ $a_0 = 0.298$, $a_1 = 1.31 \times 10^{-2}$, $a_2 = -1.81 \times 10^{-4}$, and $a_3 = 2.45 \times 10^{-6}$.

(16) GOF = $[\sum w(|F_o| - |F_c|)^2/(NO - NV)]^{1/2}$, where NO is the number of observations and NV is the number of variables.

(17) Corfield, P. W. R.; Doedens, R. J.; Ibers, J. A. *Inorg. Chem.* **1967**, *6*, 197.

(18) The major computations were performed on the USC IBM 370-155 computer by using CRYM, an amalgamated set of crystallographic programs developed by Dr. Richard Marsh's group at the California Institute of Technology.

(19) The program used for the least-squares refinement was UCIGLS, a version of W. R. Busing and H. A. Levy's ORFLS, modified by J. A. Ibers and R. J. Doedens. See R. J. Doedens in: "Crystallographic Computing"; F. R. Ahmed, Ed.; Munksgaard: Copenhagen, 1970; pp 198–200.

Table III. Anisotropic Thermal Parameters for Non-Hydrogen Atoms in Crystalline $[Ph_4P][HCr(CO)_5]$[a,b]

type[d]	B_{11}	B_{22}	B_{33}	B_{12}	B_{13}	B_{23}
Cr	3.57 (2)	3.57 (2)	2.38 (2)	0.00[c]	0.00[c]	0.00[c]
P	2.48 (2)	2.48 (2)	2.50 (3)	0.00[c]	0.00[c]	0.00[c]
O_1	5.39 (9)	5.39 (9)	2.67 (10)	0.00[c]	0.00[c]	0.00[c]
O_2	6.91 (12)	8.61 (14)	10.21 (18)	3.58 (11)	2.77 (12)	1.51 (12)
C_1	3.62 (9)	3.62 (9)	2.72 (12)	0.00[c]	0.00[c]	0.00[c]
C_2	4.86 (10)	5.56 (11)	4.36 (10)	0.69 (9)	1.08 (8)	0.79 (8)
C_{p1}	2.44 (5)	3.29 (6)	2.72 (6)	−0.15 (4)	0.10 (4)	−0.18 (5)
C_{p2}	3.27 (7)	3.71 (7)	4.05 (8)	0.41 (6)	0.44 (6)	−0.10 (6)
C_{p3}	3.28 (7)	5.56 (11)	5.57 (12)	0.67 (7)	0.92 (8)	−0.85 (9)
C_{p4}	3.35 (8)	7.12 (14)	3.88 (9)	−0.95 (9)	0.95 (7)	−1.00 (9)
C_{p5}	4.04 (9)	6.48 (13)	3.28 (8)	−1.07 (8)	0.55 (7)	0.52 (8)
C_{p6}	3.44 (7)	4.72 (9)	3.37 (7)	−0.04 (6)	0.23 (6)	0.78 (6)

[a] The numbers in parentheses are the estimated standard deviations in the last significant digits. [b] The form of the anisotropic thermal parameter is given in ref 11. [c] This is a symmetry-required value and is listed without a standard deviation. [d] Atoms are labeled in agreement with Figure 1.

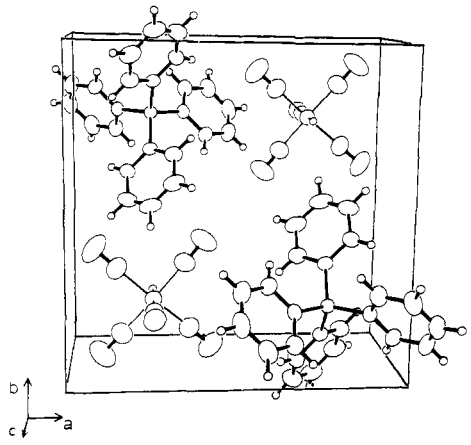

Figure 2. Unit cell of $Ph_4P^+HCr(CO)_5^-$.

culated on the basis of sp^2 geometry of the phenyl carbon atoms and with the assumption of a C-H bond distance of 1.084 Å. Each calculated phenyl hydrogen was then assigned a temperature factor equal to 1 plus the temperature factor of the carbon to which it is attached. These parameters were not refined but were added to the structure, yielding agreement factors of $R = 0.071$ and $R_w = 0.081$.

The hydrogen atoms of the borohydride group were successfully located by the low-angle-data method of LaPlaca and Ibers.[20] Data with a 2θ maximum of 33° (1548 reflections) were used with the refined atomic parameters to calculate a new difference-Fourier map. The peaks due to the four hydrogen atoms became apparent in this map. Those hydrogen positions and their isotropic thermal parameters were then refined for six cycles by using the low-angle data. These H positions were then refined several more times with use of the entire data set to yield stable positions and thermal parameters. The final agreement factors were $R = 0.066$ and $R_w = 0.074$.

Listings of structure factor amplitudes for both structures are available as supplementary material as are the ORTEP plots of the cations of both salts. The supplementary material also contains bond lengths and angles of the PPN^+ cation.

Results

Solid-State Characterization of $Ph_4P^+HCr(CO)_5^-$. The atomic coordinates and thermal parameters for $Ph_4P^+HCr(CO)_5^-$ may be found in Tables II and III, respectively. Bond lengths and bond angles are reported in Table IV. The hydride was located by difference Fourier analysis, and an ORTEP plot of the isolated anion (Figure 1) shows the pseudooctahedral symmetry as expected. Figure 2 illustrates the packing of ions in one unit cell. There are no short interanion or intercation contacts. The shortest anion–cation C–C distance is 3.510 Å between C_1 and four C_{p3} atoms which are all equidistant. Internal distances and angles are normal for the cation.[21]

Table IV. Bond Lengths and Bond Angles in Crystalline $[Ph_4P][HCr(CO)_5]$[a]

type[b]	length, Å	type[b]	length, Å
$Cr-C_1$	1.852 (4)	O_1-C_1	1.152 (5)
$Cr-C_2$	1.865 (3)	O_2-C_2	1.145 (4)
Cr-H	1.66 (5)	$P-C_{p1}$	1.791 (2)
$C_{p1}-C_{p2}$	1.384 (3)	$C_{p2}-H_{p2}$	0.92 (3)
$C_{p1}-C_{p6}$	1.401 (3)	$C_{p3}-H_{p3}$	0.95 (3)
$C_{p2}-C_{p3}$	1.393 (3)	$C_{p4}-H_{p4}$	0.95 (3)
$C_{p3}-C_{p4}$	1.372 (4)	$C_{p5}-H_{p5}$	0.94 (3)
$C_{p4}-C_{p5}$	1.376 (4)	$C_{p6}-H_{p6}$	0.99 (3)
$C_{p5}-C_{p6}$	1.385 (3)		

type[b]	angle, deg	type	angle, deg
C_1CrC_2	95.4 (1)	C_1CrH	180 (-)[c]
C_2CrC_2' [d]	89.5 (2)	C_2CrC_2'' [d]	169.2 (2)
C_2CrH	84.6 (10)		
$C_{p1}PC_{p1}'$ [d]	111.0 (1)	$C_{p1}C_{p2}H_{p2}$	120 (2)
$C_{p1}PC_{p1}''$ [d]	106.4 (1)	$C_{p3}C_{p2}H_{p2}$	120 (2)
CrC_1O_1	179.9 (2)	$C_{p2}C_{p3}H_{p3}$	121 (2)
CrC_2O_2	178.1 (2)	$C_{p4}C_{p3}H_{p3}$	118 (2)
$PC_{p1}C_{p2}$	122.0 (1)	$C_{p3}C_{p4}H_{p4}$	121 (2)
$PC_{p1}C_{p6}$	118.1 (1)	$C_{p5}C_{p4}H_{p4}$	119 (2)
$C_{p2}C_{p1}C_{p6}$	120.0 (2)	$C_{p4}C_{p5}H_{p5}$	121 (2)
$C_{p1}C_{p2}C_{p3}$	119.2 (2)	$C_{p6}C_{p5}H_{p5}$	119 (2)
$C_{p2}C_{p3}C_{p4}$	120.7 (2)	$C_{p5}C_{p6}H_{p6}$	120 (1)
$C_{p3}C_{p4}C_{p5}$	120.3 (2)	$C_{p1}C_{p6}H_{p6}$	120 (1)
$C_{p4}C_{p5}C_{p6}$	120.1 (2)		
$C_{p5}C_{p6}C_{p1}$	119.7 (2)		

[a] The numbers in parentheses are the estimated standard deviations in the last significant digits. [b] Atoms are labeled in agreement with Figure 1. [c] This is a symmetry-required value and is listed without a standard deviation. [d] For the anion, atoms labeled with a prime (') (refer to the ORTEP plot in Figure 2) are related to nonprimed atoms by the symmetry operation $^1/_2 - y, x, z$, where x, y, z are the atomic coordinates given in the tables; double-primed (") and triple-primed (''') atoms are related to nonprimed atoms by the symmetry operations $^1/_2 - x, ^1/_2 - y, z$ and $y, ^1/_2 - x, z$, respectively. For the cation, atoms labeled with a prime are related to nonprimed atoms by the symmetry operation $1 - y, -^1/_2 + x, -z$; double-primed and triple-primed atom are related to nonprimed atoms by the symmetry operations $^3/_2 - x, ^1/_2 - y, z$ and $^1/_2 + y, 1 - x, -z$, respectively.

All Cr–CO linkages in $HCr(CO)_5^-$ were found to be linear, and the CO groups cis to the hydride are required by crystallographic symmetry to be identical. A small trans effect of the hydride ligand was observed in that the bond distance of $Cr-C_{trans}$ is 1.852 (4) Å, slightly shorter than the $Cr-C_{cis}$ distance of 1.865 (4) Å. The hydride ligand was located 1.66 (5) Å from the Cr atom. Although the equatorial (cis) carbonyls are at 90° angles to each other, the $(CO)_{trans}-Cr-(CO)_{cis}$ bond angle of 95.4° indicates the

(20) (a) LaPlaca, S. J.; Ibers, J. A. *J. Am. Chem. Soc.* **1963**, *85*, 3501. (b) LaPlaca, S. J.; Ibers, J. A. *Acta Crystallogr.* **1965**, *18*, 511.

(21) Churchill, M. R.; Cooke, J. *J. Chem. Soc. A* **1970**, 2046.

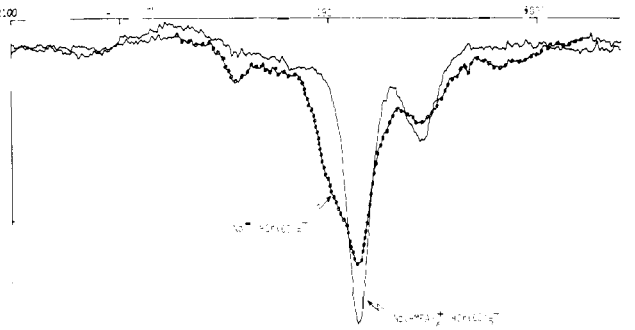

Figure 3. ν(CO) IR spectra of $HCr(CO)_5^-$: (-O-O-) spectrum of the Na^+ salt in THF; (—) spectrum upon addition of 10 equiv of HMPA. The latter puts the anion in a symmetrical solvent environment and the IR spectrum is identical with that of $PPN^+HCr(CO)_5^-$ and PPh_4^+-$HCr(CO)_5^-$ in THF.

bending of equatorial CO groups toward the hydride ligand is substantial. An alternate expression of this phenomenon is that the Cr atom is displaced toward C_1 by 0.176 Å from the plane defined by C_2, C_2', C_2'', and C_2'''.

Spectroscopic Characterization of $HCr(CO)_5^-$ in Solution. The ν(CO) IR spectra of $HCr(CO)_5^-$ as PPN^+ or Ph_4P^+ salts show only two absorptions (at normal IR concentrations (0.005 M)) at 1889 (s) and 1860 (m) cm^{-1}. These absorptions are respectively assigned to the E and A_1^1 stretching vibrational modes under C_{4v} symmetry. The third expected A_1^2 band (2020 cm^{-1}) is of very low intensity and is observed only at high concentrations (ca. 0.05 M).[22]

Equations 6 and 7 express the relationship between measured

$$I_1(A_1^1) = [(\mu'_{MCO}(1))L_{11} + 2(\cos\theta + \rho)(\mu'_{MCO}(2))L_{21}]^2 \quad (6)$$

$$I_2(A_1^2) = [(\mu'_{MCO}(1))L_{12} + 2(\cos\theta + \rho)(\mu'_{MCO}(2))L_{22}]^2 \quad (7)$$

intensities of the A_1^2 and A_1^1 bands to (1) MCO group dipole moment derivatives, μ'_{MCO}, (2) coupling between the two A_1 ν(CO) vibrations as expressed by L_{ij} matrix elements, (3) θ, the angle of the $(OC)_{ax}$–M–$(CO)_{eq}$ arrangement, and (4) the ρ parameter, which denotes electronic migration along, in this case, the fourfold axis or a transverse dipole moment change in the M–substituent ligand bond.[23] As discussed previously, this latter contribution to intensity is taken as zero for ligands presumed to have no π character such as the hydride ligand.[24] If the further assumption is made that the group dipole moments are approximately equal, the relative ratio of $I_1(A_1^1)/I_2(A_1^2)$ may be derived and rearranged as in eq 8. The following values of the L_{ij} coupling elements were

$$\cos\theta = \tfrac{1}{2}\left(\frac{I_{ratio}^{1/2}L_{11} - L_{12}}{L_{22} - I_{ratio}^{1/2}L_{21}}\right) \quad (8)$$

used: $L_{12} = -L_{21} = 0.09978$; $L_{11} = L_{22} = 0.3686$.[25,26] The square root of the measured intensity ratio was 0.0938. The angle θ was calculated to be 94.9°.

The ν(CO) IR spectrum of $Na^+HCr(CO)_5^-$ in THF showed bands in addition to those of Ph_4P^+ or $PPN^+HCr(CO)_5^-$. A prominent shoulder was on the high-frequency side of the E vibrational mode, and the A_1^1 band was poorly resolved (Figure 3). On addition of hexamethylphosphoric triamide (HMPA, ca. 10 equiv) the spectrum of C_{4v} $HCr(CO)_5^-$, identical with that of $Ph_4P^+HCr(CO)_5^-$ in THF, was obtained.

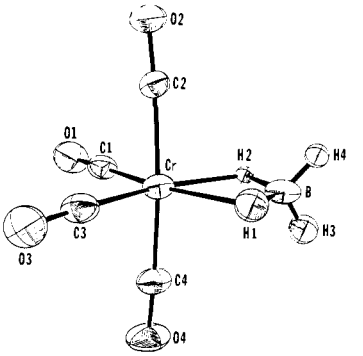

Figure 4. Plot of the $(\mu\text{-}H)_2BH_2Cr(CO)_4^-$ anion. Thermal ellipsoids show 25% probability.

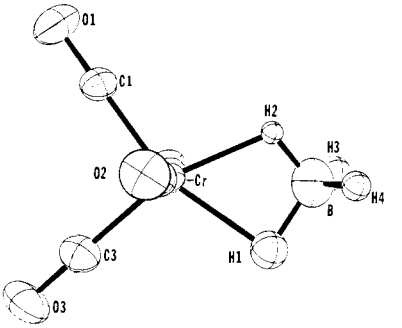

Figure 5. View of $(\mu\text{-}H)_2BH_2Cr(CO)_4^-$ collinear with the axial CO groups, which shows the asymmetry of the $(\mu\text{-}H)_2B$ unit. Thermal ellipsoids show 25% probability.

Such a salt effect was not detected by the ^1H NMR spectrum. At −50 °C and at room temperature the hydride resonance of $HCr(CO)_5^-$ in THF solution was 6.92 ppm upfield from Me_4Si regardless of counterion, i.e., Na^+, PPN^+, or Ph_4P^+.

Reactions of $HCr(CO)_5^-$ with BH_3. Within 15 min after addition of 0.15 mmol of BH_3-THF to a THF solution of 0.068 mmol of $PPN^+HCr(CO)_5^-$ at room temperature IR bands at 1835, 1925, and 1945 cm^{-1} were apparent in addition to those of the starting material at 1889 and 1860 cm^{-1}. Upon 2 h of stirring, the band at 1860 cm^{-1} was gone and the band at 1925 cm^{-1} had decreased substantially in intensity relative to those at 1836 and 1942 cm^{-1}. From the growth pattern it was clear that the 1835- and 1945-cm^{-1} bands belonged to different species and the predominant appearing species was then possessing the 1835-cm^{-1} absorbance. At this point the weak bands above 2000 cm^{-1} were clearly discernible at 2011 and 2032 cm^{-1}. After 4 h the 1925-cm^{-1} band was no longer observable and the spectrum was interpreted to be a mixture of only two species, $(\mu\text{-}H)[Cr(CO)_5]_2^-$ (ν(CO) = 2033 w, 1945 s, and 1886 m cm^{-1}) and $(\mu\text{-}H)_2BH_2Cr(CO)_4^-$ (ν(CO) = 2011 w, 1884 br, s, and 1835 m cm^{-1}). A similar experiment carried out at 0 °C yielded only $(\mu\text{-}H)[Cr(CO)_5]_2^-$, as did a room-temperature experiment using $AlMe_3$ instead of BH_3 as the Lewis acid.

Solid-State Characterization of $PPN^+(\mu\text{-}H)_2BH_2Cr(CO)_4^-$. The atomic and thermal parameters for $PPN^+Cr(CO)_4BH_4^-$ are given in Tables V and VI. The bond distances and angles found for the anion are in Table VII. Two views are given by the ORTEP plots in Figures 4 and 5.

The environment about the Cr atom is that of a distorted octahedron. The axial carbonyls are slightly bent away from the borohydride ligand, ∠C(2)–Cr–C(4) = 175.6°. The small bite of the bidentate borohydride ligand leads to the H(1)–Cr–H(2) angle of 58° and allows the equatorial carbonyls to open somewhat, ∠C(1)–Cr–C(3) = 94.8°. The C(1)–Cr–H(2) and C(3)–Cr–H(1) angles are the same within the experimental error of this analysis. The atoms in the equatorial plane (Cr, C(1), C(3), H(1), H(2)) are coplanar within ±0.02 Å. The boron atom lies outside the

(22) See Figure 1 in ref 2a.
(23) Darensbourg, D. J.; Brown, T. L. *Inorg. Chem.* **1968**, *7*, 959. Darensbourg, D. J. *Inorg. Chim. Acta* **1970**, *4*, 597.
(24) Darensbourg, M. Y.; Darensbourg, D. J.; Barros, H. L. C. *Inorg. Chem.* **1978**, *17*, 297. Bor, G. *Inorg. Chim. Acta* **1967**, *1*, 81.
(25) The L_{ij} matrix elements were derived from a Cotton-Kraihanzel[26] restricted force field force constant calculation. The force constants themselves were very slightly different from those reported earlier[2a] for $Et_4N^+HCr(CO)_5^-$ due to small (±3 cm^{-1}) frequency differences in the IR spectra. For Ph_4P^+-$HCr(CO)_5^-$, k_1(axial CO) = 14.15 mdyn/Å and k_2(equatorial CO) = 15.05 mydn/Å.
(26) Cotton, F. A.; Kraihanzel, C. S. *J. Am. Chem. Soc.* **1962**, *84*, 4432.

Table V. Atomic Coordinates for Crystalline [PPN][$Cr(CO)_4BH_4$][a,b]

atom	x	y	z	atom	x	y	z
Cr	0.17086 (12)	0.22141 (10)	0.85363 (12)	C(24)	0.8935 (10)	0.5033 (8)	0.8149 (10)
C(1)	0.2489 (8)	0.3137 (7)	0.9203 (7)	C(25)	0.8063 (9)	0.4464 (7)	0.8019 (9)
O(1)	0.3013 (7)	0.3712 (5)	0.9628 (6)	C(30)	0.5054 (8)	0.4315 (6)	0.7203 (8)
C(2)	0.0386 (8)	0.2918 (6)	0.9448 (7)	C(31)	0.4965 (11)	0.5075 (8)	0.8198 (10)
O(2)	−0.0402 (6)	0.3403 (4)	1.0010 (5)	C(32)	0.3848 (12)	0.5651 (9)	0.8597 (11)
C(3)	0.1181 (8)	0.2763 (7)	0.7288 (8)	C(33)	0.2881 (11)	0.5484 (9)	0.8015 (11)
O(3)	0.0866 (7)	0.3094 (5)	0.6463 (6)	C(34)	0.2919 (11)	0.4699 (9)	0.7020 (11)
C(4)	0.3050 (9)	0.1606 (7)	0.7636 (8)	C(35)	0.4040 (10)	0.4124 (8)	0.6618 (9)
O(4)	0.3889 (7)	0.1270 (6)	0.7067 (7)	C(40)	0.7119 (8)	0.1048 (6)	0.4857 (7)
B	0.1678 (11)	0.0818 (9)	0.9150 (10)	C(41)	0.8189 (9)	0.0416 (7)	0.4597 (8)
H(1)	0.113 (7)	0.103 (5)	0.826 (7)	C(42)	0.8395 (10)	−0.0448 (8)	0.5060 (10)
H(2)	0.201 (5)	0.139 (4)	0.954 (5)	C(43)	0.7494 (11)	−0.0620 (9)	0.5742 (10)
H(3)	0.230 (6)	0.032 (5)	0.900 (6)	C(44)	0.6436 (10)	0.0013 (8)	0.5971 (9)
H(4)	0.116 (6)	0.070 (5)	0.964 (6)	C(45)	0.6224 (8)	0.0870 (7)	0.5511 (8)
P(1)	0.64433 (22)	0.35562 (17)	0.67082 (20)	C(50)	0.8065 (8)	0.2213 (6)	0.3549 (8)
P(2)	0.67775 (22)	0.21701 (18)	0.43402 (20)	C(51)	0.8986 (8)	0.2512 (7)	0.4190 (8)
N	0.6376 (6)	0.3084 (5)	0.5349 (6)	C(52)	1.0034 (9)	0.2487 (7)	0.3605 (9)
C(10)	0.6801 (8)	0.2707 (6)	0.7678 (7)	C(53)	1.0141 (10)	0.2127 (8)	0.2344 (10)
C(11)	0.5940 (9)	0.2584 (7)	0.8386 (9)	C(54)	0.9225 (10)	0.1830 (8)	0.1720 (10)
C(12)	0.6226 (10)	0.1837 (8)	0.9059 (10)	C(55)	0.8156 (10)	0.1873 (8)	0.2313 (9)
C(13)	0.7326 (11)	0.1276 (8)	0.8994 (10)	C(60)	0.5617 (8)	0.2096 (6)	0.3293 (8)
C(14)	0.8223 (10)	0.1399 (8)	0.8286 (10)	C(61)	0.4835 (10)	0.2930 (8)	0.3182 (9)
C(15)	0.7928 (9)	0.2144 (7)	0.7599 (8)	C(62)	0.3910 (11)	0.2871 (9)	0.2353 (11)
C(20)	0.7508 (8)	0.4295 (7)	0.6925 (8)	C(63)	0.3829 (11)	0.1989 (9)	0.1660 (10)
C(21)	0.7744 (9)	0.4686 (7)	0.5970 (9)	C(64)	0.4596 (10)	0.1159 (8)	0.1771 (10)
C(22)	0.8620 (11)	0.5248 (9)	0.6122 (11)	C(65)	0.5536 (9)	0.1177 (7)	0.2596 (9)
C(23)	0.9184 (11)	0.5395 (9)	0.7204 (11)				

[a] Numbering scheme for the PPN^+ cation: C(10)–C(15) = phenyl (1), C(20)–C(25) = phenyl(2), etc., with phenyl(1)–phenyl(3) attached to P(1) and phenyl(4)–phenyl(6) attached to P(2); atoms are labeled for the anion according to Figure 4. [b] The numbers in parentheses are the estimated standard deviations in the last significant digits.

Table VI. Thermal Parameters for Crystalline [PPN][$Cr(CO)_4BH_4$][a,b]

(A) Anisotropic Thermal Parameters

atom[c]	$10^4\beta_{11}$	$10^4\beta_{22}$	$10^4\beta_{33}$	$10^4\beta_{12}$	$10^4\beta_{13}$	$10^4\beta_{23}$
Cr	70.6 (13)	57.8 (9)	79.5 (13)	−9.8 (9)	0.7 (10)	0.5 (8)
C(1)	97 (10)	65 (7)	71 (8)	−19 (7)	8 (7)	0.2 (6)
O(1)	162 (9)	96 (6)	129 (8)	−64 (6)	14 (7)	−8 (5)
C(2)	84 (9)	52 (6)	79 (8)	−6 (6)	−1 (7)	7 (6)
O(2)	100 (7)	75 (5)	110 (7)	0 (5)	19 (6)	6 (4)
C(3)	112 (11)	78 (8)	87 (10)	−5 (7)	1 (8)	4 (7)
O(3)	194 (10)	115 (6)	98 (7)	−4 (6)	34 (7)	30 (5)
C(4)	89 (10)	71 (10)	118 (10)	−19 (7)	19 (8)	−7 (7)
O(4)	112 (8)	115 (6)	216 (11)	−23 (6)	78 (8)	−21 (6)
B	122 (14)	81 (9)	128 (13)	−1 (9)	55 (11)	8 (9)
P(1)	67 (2)	34 (2)	50 (2)	−13 (2)	−2 (2)	5 (1)
P(2)	57 (2)	36 (2)	48 (2)	−9 (2)	−1 (2)	9 (1)

(B) Isotropic Thermal Parameters

atom[c]	B, Å^2	atom	B, Å^2	atom	B, Å^2	atom	B, Å^2
N	3.2 (2)	C(20)	3.5 (2)	C(34)	6.5 (3)	C(52)	4.2 (2)
H(1)	5 (2)	C(21)	4.4 (2)	C(35)	4.7 (2)	C(53)	5.1 (2)
H(2)	2 (1)	C(22)	6.0 (3)	C(40)	2.9 (2)	C(54)	5.4 (3)
H(3)	5 (2)	C(23)	6.0 (3)	C(41)	4.0 (2)	C(55)	4.8 (2)
H(4)	3 (2)	C(24)	5.5 (3)	C(42)	5.6 (3)	C(60)	3.0 (2)
C(10)	3.0 (2)	C(25)	4.4 (2)	C(43)	5.8 (3)	C(61)	5.0 (2)
C(11)	4.2 (2)	C(30)	3.3 (2)	C(44)	4.6 (2)	C(62)	6.7 (3)
C(12)	5.5 (3)	C(31)	5.5 (3)	C(45)	3.7 (2)	C(63)	6.0 (3)
C(13)	5.6 (3)	C(32)	6.4 (3)	C(50)	3.2 (2)	C(64)	5.1 (2)
C(14)	5.1 (2)	C(33)	6.3 (3)	C(51)	3.4 (2)	C(65)	4.4 (2)
C(15)	4.1 (2)						

[a] The numbers in parentheses are the estimated standard deviations in the last significant digits. [b] The anisotropic thermal parameter is of the form $\exp[-(\beta_{11}h^2 + \beta_{22}k^2 + \beta_{33}l^2 + \beta_{12}hk + \beta_{13}hl + \beta_{23}kl)]$. [c] Atoms are labeled according to Figure 4.

plane by −0.09 Å and is at a distance of 2.29 Å from the Cr atom.

The average Cr–C_{ax} distance is 1.86 Å, and the Cr–C_{eq} distances average to 1.81 Å with the shorter Cr–C bonds trans to the substituent hydrides. The C–O distances are identical within the experimental error. At first glance, there appears to be some asymmetry associated with the binding of the borohydride of Cr. At 1.96 (7) Å the Cr–H(1) distance is 0.16 Å longer than the Cr–H(2) distance of 1.80 (6) Å. Similarly, the B–H(b) distances differ with B–H(1) = 1.25 (8) Å and B–H(2) = 1.01 (6) Å. It is not clear, however, if these differences are meaningful, in view of the large uncertainties in the H positions.

Aside from the apparent bond length differences, the tetrahedral environment of the BH_4 group is well preserved. The two B–H(t) distances are identical, 0.90 (7) and 0.90 (7) Å. Interestingly, the boron atom is not angularly symmetrically positioned with respect to the equatorial carbonyl groups: the C(1)–Cr–B angle

Table VII. Bond Lengths and Bond Angles in Crystalline $[PPN][Cr(CO)_4BH_4]$[a,b]

	(A) Bond Lengths (Å)		
Cr-B	2.29 (1)	C(1)-O(1)	1.16 (1)
Cr-H(1)(b)	1.96 (7)	C(2)-O(2)	1.15 (1)
Cr-H(2)(b)	1.80 (6)	C(3)-O(3)	1.16 (1)
Cr···H(3)(t)	2.85 (7)	C(4)-O(4)	1.15 (1)
Cr···H(4)(t)	2.94 (7)		
Cr-C(1)(eq)	1.82 (1)	B-H(1)(b)	1.25 (8)
Cr-C(2)(ax)	1.87 (1)	B-H(2)(b)	1.01 (6)
Cr-C(3)(eq)	1.81 (1)	B-H(3)(t)	0.90 (7)
Cr-C(4)(ax)	1.85 (1)	B-H(4)(t)	0.90 (7)
	(B) Bond Angles (Deg)		
H(1)-Cr-H(2)	58 (3)	O(3)-Cr-O(4)	86.0 (2)
C(1)-Cr-H(1)	161 (2)	Cr-C(1)-O(1)	178.4 (9)
C(3)-Cr-H(2)	162 (2)	Cr-C(2)-O(2)	175.7 (8)
C(1)-Cr-H(2)	103 (2)	Cr-C(3)-O(3)	177.9 (8)
C(3)-Cr-H(1)	105 (2)	Cr-C(4)-O(4)	176.7 (10)
O(1)-Cr-H(1)	160 (2)	C(1)-Cr-B	127.6 (4)
O(3)-Cr-H(2)	162 (2)	C(3)-Cr-B	137.4 (4)
C(1)-Cr-C(2)	88.9 (4)	O(1)-Cr-B	127.2 (3)
C(1)-Cr-C(3)	94.8 (4)	O(3)-Cr-B	137.0 (3)
C(1)-Cr-C(4)	87.2 (4)	H(1)-B-H(2)	107 (5)
C(2)-Cr-C(3)	90.7 (4)	H(1)-B-H(3)	116 (6)
C(2)-Cr-C(4)	175.6 (4)	H(1)-B-H(4)	107 (6)
C(3)-Cr-C(4)	87.5 (4)	H(2)-B-H(3)	105 (6)
O(1)-Cr-O(2)	88.0 (2)	H(2)-B-H(4)	111 (6)
O(1)-Cr-O(3)	95.4 (2)	H(3)-B-H(4)	110 (7)
O(1)-Cr-O(4)	85.8 (2)	Cr-H(1)-B	89 (4)
O(2)-Cr-O(3)	90.9 (2)	Cr-H(2)-B	106 (4)
O(2)-Cr-O(4)	172.7 (2)		

[a] Atoms are labeled according to Figure 4. [b] The numbers in parentheses are the estimated standard deviations in the last significant digits.

is 127.6 (4)° and the C(3)–Cr–B angle is 137.4 (4)°.

Similar to most,[27] but not all,[28] PPN^+ cation structure determinations, the P–N–P framework is bent (146.6 (30)°), the P–N bond lengths are 1.56 (6) Å, and the phenyl rings are substantially eclipsed.

Spectroscopic Characterization of $(\mu\text{-}H)_2BH_2Cr(CO)_4^-$ in Solution. Although a four-band carbonyl stretching pattern is expected for a species of approximate C_{2v} symmetry such as $(\mu\text{-}H)_2BH_2Cr(CO)_4^-$, only three absorptions are observed in the solution and solid-state (Nujol mull) spectra of the anion (ν(CO) = 2011 w, 1884 br, s, and 1835 m cm^{-1}). Since in the isostructural $(\mu\text{-}H)_2BH_2Mo(CO)_4^-$ the two central bands are close in frequency (i.e., 2020 w, 1900 s, 1878 m, and 1810 m cm^{-1}),[10] it is reasonable to assume that the broad band centered at 1884 cm^{-1} is a combination of two degenerate vibrational modes.

The proton NMR spectrum in THF-d_8 showed only one resonance in the temperature range of −80° to +50 °C, at 9.5 ppm upfield from Me_4Si. At the higher temperatures the features of a quartet are clearly imposed on the broad band, and its center is at the same position as the center of the featureless band at −80 °C. We were unable to obtain the boron-decoupled spectrum.

The carbon-13 NMR spectrum of $PPN^+(\mu\text{-}H)_2BH_2Cr(CO)_4^-$ exhibited two resonances of equal intensities in THF, at 217.4 and 230.6 ppm downfield from Me_4Si. These peaks were invariant with temperature (−60, 0, and +30 °C).

Reaction of $(\mu\text{-}H)_2BH_2Cr(CO)_4^-$ with CO. THF solutions of $PPN^+(\mu\text{-}H)_2BH_2Cr(CO)_4^-$ were cooled to −78 °C, degassed, and back-filled with CO. Infrared spectra taken of samples immediately after agitation and warming to room temperature showed diminishing of the borohydride complex and IR bands characteristic of the species $HCr(CO)_5^-$ and $(\mu\text{-}H)[Cr(CO)_5]_2^-$. The mononuclear hydride initially predominated. After 15 min at room temperature the reactant was completely gone and the two products were present in roughly equal amounts.

Scheme IV

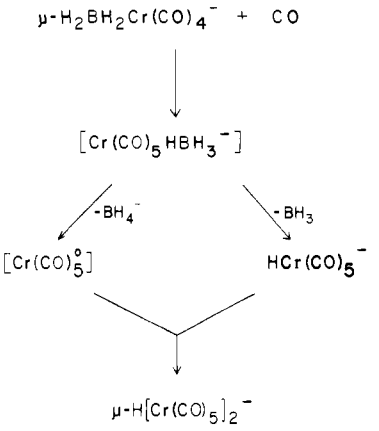

Discussion

A structural feature common to all mononuclear $HM(CO)_x$ species is the bending of CO groups cis to the hydride toward that site. This feature prevails in solution according to infrared intensity studies such as that presented above for $HCr(CO)_5^-$ (C_{ax}–M–C_{eq} angle calculated at 94.9°), and as presented previously for $HCo(CO)_4$ (calcd 101°),[24] $HMn(CO)_5$ (calcd 96.5°),[29] and $HFe(CO)_4^-$ (calcd 100.2°).[24] As determined by more direct methods, the C_{ax}–M–C_{eq} angles for the C_{3v} species $HCo(CO)_4$ and $HFe(CO)_4^-$ are 99.7 (6)[8] and 99.1° (average value),[30] respectively. For the pseudooctahedral species $HMn(CO)_5$ and $HCr(CO)_5^-$ the analogous angles are 94.5 (9)[8] and 95.4 (1)°, respectively. The values listed for $HFe(CO)_4^-$ and $HCr(CO)_5^-$ are taken from X-ray diffraction data, and for $HCo(CO)_4$ and $HMn(CO)_5$, from gas-phase electron diffraction data. The electron diffraction results for $HMn(CO)_5$ were quite similar to the solid-state (X-ray and neutron diffraction) structure determinations of both the α and β forms of $HMn(CO)_5$.[31]

Yet another common structural feature of $HMn(CO)_5$ and $HCr(CO)_5^-$ is that the trans M–C bond distance is only slightly shorter, if not statistically indistinguishable in the manganese studies, from the average cis M–C bond distance. For $HCr(CO)_5^-$ the difference is only 0.01 Å. The CO groups are certainly electronically different as shown by their stretching force constants.[25] The ν(CO) spectrum of the Na^+ salt (Figure 3) is interpreted to represent a mixture of solvent-separated and contact ion pairs in which the contact is between Na^+ and the oxygen of the CO group of lower force constant, i.e., the axial CO. This interpretation is analogous to that of *trans*-$Ph_3PV(CO)_4CO\cdots Na^+$.[32] (It is possible that a minor amount of $Na^+/HCr(CO)_5^-$ contact interaction is with the hydride ligand itself.) The small solid-state structural trans effect contrasts sharply with that of other $LM(CO)_5$ structures containing such disparate ligand types as X^-,[33] PR_3,[34] and O-donor ligands.[35] In these cases the trans M–C bond distance is from 0.02 to 0.08 Å shorter than is the cis M–C bond.

The lack of a significant structural trans effect of the hydride ligand in mononuclear hydrides is similar to compounds involving other σ-donor ligands such as CH_3 and SnR_3;[8] however, it does not extend to bridging hydride systems such as $(\mu\text{-}H)[Cr(CO)_5]_2^-$. In these cases the $Cr(CO)_5$ moiety is in a strict octahedral setting ($\angle C_{ax}$–Cr–$C_{eq} \simeq 90°$). The neutron diffraction study of $Et_4N^+(\mu\text{-}H)[Cr(CO)_5]_2^-$ found the Cr–C_{ax} bond length to be 1.827

(27) Handy, L. B.; Ruff, J. K.; Dahl, L. F. *J. Am. Chem. Soc.* **1970**, *92*, 7327. Bau, R.; Wilson, R. D. *Ibid.* **1974**, *96*, 7601.
(28) Kirtley, S. W.; Chanton, J. P.; Love, R. A.; Tipton, D. L.; Sorrel, T. N.; Bau, R. *J. Am. Chem. Soc.* **1980**, *102*, 3451.
(29) Braterman, P. S.; Bau, R.; Kaesz, H. D. *Inorg. Chem.* **1967**, *68* 2097.
(30) Bau, R.; Smith, M. B. *J. Am. Chem. Soc.* **1973**, *95*, 2388.
(31) LaPlaca, S. J.; Hamilton, W. C.; Ibers, J. A.; Davison, A. *Inorg. Chem.* **1969**, *8*, 1928.
(32) Darensbourg, M. Y.; Hanckel, J. M. *J. Organomet. Chem.* **1981**, *217*, C9. Darensbourg, M. Y.; Hanckel, J. M. *Organometallics* **1982**, *1*, 82.
(33) Burschka, V.; Schenk, W. A. *Z. Anorg. Allg. Chem.* **1981**, *477*, 149. Calhoun, H. P.; Trotter, J. *J. Chem. Soc., Dalton Trans.* **1974**, 377.
(34) Cotton, F. A.; Darensbourg, D. J.; Ilsley, W. H. *Inorg. Chem.* **1981**, *20*, 578.
(35) Cotton, F. A.; Darensbourg, D. J.; Kolthammer, B. W. S. *J. Am. Chem. Soc.* **1981**, *103*, 398.

(3) Å, and the Cr–C_{eq} distances averaged to 1.898 (3) Å.[36] A symmetrical but angular hydride bridge bond (∠Cr–H–Cr = 158.9 (6)°) and some M–M interaction[37] completed the coordination sphere of each $Cr(CO)_5$ unit. The structure determination of $HCr(CO)_5^-$ provides an opportunity to compare an M–H(t) distance with an M–H(b) distance in a non- (or lightly) supported bridging hydride dimer. Surprisingly there is no significant difference in the Cr–H(t) bond distance of $HCr(CO)_5^-$ (1.66 (5) Å, X-ray analysis) and in the average Cr–H(b) distance of $(\mu\text{-H})[Cr_2(CO)_{10}]^-$ (1.722 (20) Å, neutron analysis[36]). In contrast, the bridging hydride distance lengthens substantially in the mixed-metal bridging hydride situation of $(\mu\text{-H})_2BH_2Cr(CO)_4^-$ (average Cr–H(b) = 1.88 (7) Å).

$(\mu\text{-H})_2BH_2Cr(CO)_4^-$ shows some asymmetry in the Cr–C_{ax} and Cr–C_{eq} bond lengths. As expected, the Cr–C bonds of the CO groups trans to each other appear to be the longer ones. As noted above, in contrast to the case for $HCr(CO)_5^-$ and $(\mu\text{-H})[Cr(CO)_5]_2^-$, the axial CO groups of $(\mu\text{-H})_2BH_2Cr(CO)_4^-$ bend away from the bridging hydride sites. The small bite angle of the borohydride allows the C_{eq}–Cr–C_{eq} angle to expand to ca. 95°. This latter result constitutes the substantial difference between the structure of this anion and its Mo analogue.[10] Despite the larger size of the Mo atom, in $(\mu\text{-H})_2BH_2Mo(CO)_4^-$ the C_{eq}–Mo–C_{eq} angle actually closes to 84.5 (5)° while the H(b)-Mo-H(b) angle is only 59°, as in the Cr derivative. Also similar to the Mo derivative, the boron is displaced away from the bisector of the C(1)–Cr–C(3) angle, yielding different Cr–H(b)–B angles (∠Cr–H(2)–B = 106 (4)° and ∠Cr–H(2)–B = 89 (4)°). Kirtley, Bau, Marks, et al.[10] noted that the sum of the estimated covalent radii of Mo and B was greater than the observed Mo–B distance in $(\mu\text{-H})_2BH_2Mo(CO)_4^-$. Likewise, with the assumption of the covalent radius of Cr to be on the order of 1.48 Å (half the Cr–Cr distance in $Cr_2(CO)_{10}^{2-}$)[38] and that of B to be 0.88 Å,[39] their sum of 2.36 Å is again apparently larger than the observed Cr–B distance of 2.29 (1) Å. Thus we view one of the Cr–H–B bridges as a "typical" tight hydride-bridged binuclear system involving some M–M'[37] or M–M'[40] interaction concomitant with the angular hydride bridges in the closed three-center, two-electron bonding mode, A.[41] The requirement for hexacoordination and the proximity of a $B^{\delta+}$–$H^{\delta-}$ unit completes the coordination sphere, yielding a long B–H(b) bond as in B.

A

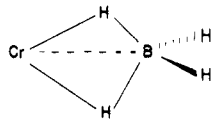

B

Relative to the NMR time scale, rapid H(b)–H(t) interchange occurred at the lowest temperature investigated, −80 °C. In contrast, $(\mu\text{-H})_2BH_2Mo(CO)_4^-$ showed separate resonances of H(b) and H(t) at −60 °C with coalescence at −35 °C.[10] Similar to the analogous study carried out on $(\mu\text{-H})_2BH_2Mo(Co)_4^-$ it is clear that a rearrangement of the axial and equatorial CO groups (^{13}C NMR, VT study) does not coincide with the bridge hydrogen–terminal hydrogen interchange (^1H NMR, VT study) as one might expect[10] were the five-coordinate $H_3B(\mu\text{-H})Cr(CO)_4^-$ an intermediate in the simplest possible mechanism for intramolecular hydrogen exchange: bridge opening, rotation of BH_3 unit, bridge closing.[42] The observations of the fluxional BH_4^- ligand concurrent with rigid $M(CO)_4$ units do not definitely rule out the five-coordinate intermediate; however, it does say that $(CO)_{ax}$–$(CO)_{eq}$ interchange cannot occur at the same rate, in the same process, as the H(t)–H(b) interchange.[43,44] This simplest possible mechanism for BH_4^- fluxionality has been quite clearly established in $HRu[(\mu\text{-H})_2BH_2]tpp$ (tpp = $Ph_2P(CH_2CH_2CH_2PPh_2)_2$), which presents a stereochemically rigid structure at room temperature. The two types of Ru–H(b)–B bridging hydrides (one trans to Ru–H(t) and the other trans to a P donor atom) show different barriers to bridge hydrogen–terminal hydrogen atom interchange.[45]

In view of the rigid nature of the $M(CO)_4$ units of both species we are inclined to promote the idea that H(b)–M bond breakage is accompanied by H(t)–M bond making in a concerted fashion, localized at the two original borohydride coordination sites and permuting no other carbonyl coordination sites. This is in effect the mechanism of eq 15 in ref 10. Finally, with regard to the NMR studies we note that, in contrast to the case for the carbonyl portion of $(\mu\text{-H})_2BH_2Cr(CO)_4^-$, in $HCr(CO)_5^-$ (but *not* $HMo(CO)_5^-$) there is rapid interchange of $(CO)_{trans}$–$(CO)_{cis}$ at temperatures >0 °C.[2] Clearly the bidentate nature of the borohydride ligand, or the delocalized nature of the $(\mu\text{-H})_2B$ ligand unit, restricts the fluxionality of the coordination sphere.

Reaction of $(\mu\text{-H})_2BH_2Cr(CO)_4$ with CO again indicates the bridge-opening possibility. The production of two products, $HCr(CO)_5^-$ and $(\mu\text{-H})[Cr(CO)_5]_2^-$, is explained by the application of chemistry found in Scheme II according to Scheme IV. As presented above (Results section) all of the steps of Scheme IV have been shown to be reversible with the exception of the combination of 16-electron $[Cr(CO)_5^0]$ with $HCr(CO)_5^-$ to produce the very stable binuclear hydride. We have been unable to measure the extremely fast rate with which the dimer formation occurs and can only add in this regard that addition of a mixture of BH_3·THF and photochemically produced $Cr(CO)_5$·THF in THF to a THF solution of $HCr(CO)_5^-$ yielded on time of mixing only $(\mu\text{-H})[Cr(CO)_5]_2^-$. That is, the THF adduct of the $Cr(CO)_5^0$ Lewis acid competed more effectively for $HCr(CO)_5^-$ than did the THF adduct of the main-group-element Lewis acid.

The monodentate borohydride complex in Schemes II and IV has not been identified. A transient band at ca. 1925 cm^{-1} was observed in the preparation of $HCr(CO)_5^-$ via the BH_4^- hydride donor route (eq 2), in the reaction of BH_3 with $HCr(CO)_5^-$, and also in the reaction of CO with $(\mu\text{-H})_2BH_2Cr(CO)_4^-$. It is possible that this band represents the monodentate borohydride derivative $H_3B(\mu\text{-H})Cr(CO)_5^-$;[46] however, further experimental corroboration is needed.

Acknowledgment. This work was supported by the National Science Foundation, Grant Nos. CHE 79-23204 (M.Y.D.) and

(36) Roziere, J.; Williams, J. M.; Stewart, R. P., Jr.; Peterson, J. L.; Dahl, L. F. *J. Am. Chem. Soc.* **1977**, *99*, 4497.
(37) Darensbourg, D. J.; Burch, R. R., Jr.; Darensbourg, M. Y. *Inorg. Chem.* **1978**, *17*, 2677.
(38) Handy, L. B.; Ruff, J. K.; Dahl, L. F. *J. Am. Chem. Soc.* **1970**, *92*, 7312.
(39) Pauling, L. "The Nature of the Chemical Bond"; Cornell University Press: Ithaca, NY, 1960; p 246.
(40) Tebbe, F. N.; Guggenberger, L. J. *J. Chem. Soc., Chem. Commun.* **1973**, 227. Crotty, D. E.; Anderson, T. J.; Glick, M. D.; Oliver, J. P. *Inorg. Chem.* **1977**, *16*, 2436. Porai-Koshits, M. A.; Antsyshkina, A. S.; Pasynskii, A. A.; Sadikov, G. G.; Skripkin, Yu. V.; Ostrikova, V. N. *Inorg. Chim. Acta* **1979**, *34*, L285.
(41) Bau, R.; Teller, R. G.; Kirtley, S. W.; Koetzle, T. F. *Acc. Chem. Res.* **1979**, *12*, 176. Bau, R.; Koetzle, T. F. *Pure Appl. Chem.* **1978**, *50*, 55.
(42) Although we did not check for an intermolecular BH_4^- exchange, the concentration dependence of the fluxional process was determined in the analogous Mo study.[10] No dependence was observed.
(43) Although five-coordinate metal carbonyls and derivatives are generally structurally nonrigid on the NMR time scale, it is possible that the $(CO)_{ax}$–$(CO)_{eq}$ exchange occurs slower than the BH_4^- ring closing. Such was the case for $M(CO)_4(\eta^4\text{-norbornadiene})$.[44] Stereospecific labeling studies allowed for a kinetic study of $(CO)_{ax}$–$(CO)_{eq}$ equilibration, and a separate kinetic study established the activation barrier to the ring closing process in the five-coordinate intermediate $M(CO)_4(\eta^2\text{-norbornadiene})$. The barrier for the former process was greater than for the latter. It should be noted that in both types of molecules, $(\mu\text{-H})_2BH_2M(CO)_4^-$ and $M(CO)_4(\eta^4\text{-norbornadiene})$, the more stable form of the five-coordinate intermediate is afforded on ring opening. That is, the unique ligand occupies the equatorial site in the square pyramid.
(44) Darensbourg, D. J.; Nelson, H. H., III; Murphy, M. A. *J. Am. Chem. Soc.* **1977**, *99*, 896.
(45) Letts, J. B.; Mazanec, T. J.; Meek, D. W. *J. Am. Chem. Soc.* **1982**, *104*, 3898.
(46) Monodentate borohydride complexes are in fact known for other metals, and in at least one case this has been crystallographically verified: Takusagawa, F.; Fumagalli, A.; Koetzle, T. F.; Shore, S. G.; Schmitkons, T.; Fratini, A. V.; Morse, K. W.; Wei, C.-Y.; Bau, R. *J. Am. Chem. Soc.* **1981**, *103*, 5165.

CHE 79-26479 (R.B.).

Registry No. $Na^+HCr(CO)_5^-$, 83399-32-0; $Na_2Cr(CO)_5$, 52154-81-1; $PPN^+Cr(CO)_5I^-$, 39048-35-6; $PPN^+(\mu\text{-}H)_2BH_2Cr(CO)_4^-$, 83399-34-2; $Ph_4P^+HCr(CO)_5^-$, 83399-35-3; $Cr(CO)_5(NC_5H_{11})$, 15710-39-1; $(\mu\text{-}H)[Cr(CO)_5]_2^-$, 19571-06-3.

Supplementary Material Available: Listings of the structure factor amplitudes for both structures as well as bond lengths and bond angles of the PPN^+ cation and ORTEP plots of the cations of both salts (28 pages). Ordering information is given on any current masthead page.

Phosphinonitrene, Phosphazene, and Aminophosphinidene. Structures and Stabilities

Georges Trinquier

Contribution from the Laboratoire de Physique Quantique (ERA 821), Université Paul Sabatier, 31062 Toulouse Cedex, France. *Received February 25, 1982*

Abstract: Singlet and triplet H_2PN isomers are investigated through ab initio effective potential calculations using double-ζ + polarization basis sets; electron correlation is included. All singlet states are planar, indicating conjugation of the amino and phosphino π lone pairs in H_2N–P and H_2P–N, respectively. The corresponding triplet states show pyramidalized amino and phosphino groups. The calculated thermodynamic stability ordering for all isomers is HP=NH $^1A'$ (trans) $\simeq$ H_2N—P $^3A''$ $\simeq$ HP=NH $^1A'$ (cis) < H_2N—P $^1A_1$ $\ll$ HP—NH ^3A < H_2P—N $^1A_1$ < H_2P—N $^3A''$, corresponding to relative energies 0, 7, 28, 41, and 47 kcal/mol, respectively. The structure of singlet phosphinonitrene supports the phosphonitrile notation $H_2P{\equiv}N$, due to delocalization of the lone pairs $n_\pi(P) \rightarrow p_\pi(N)$ and $n_\pi(N) \rightarrow d_\pi(P)$. The structure of singlet aminophosphinidene shows less multiple character in the NP bond $H_2N{=}P$. The π contribution to the PN bond energy in HP=NH is estimated at about 40 kcal/mol. Cis/trans isomerization of HP=NH proceeds via a linear PNH configuration with an energy barrier of 15 kcal/mol.

Introduction

The number of compounds of dicoordinated phosphorus(III) involving a –P=N– double bond is fairly limited to date. However, they are becoming more and more numerous either in cyclic forms or noncyclic forms, the P=N bond being either conjugated or nonconjugated.[1-5] Some X-ray data[6-8] are now available. In a compound like R—P=N—R′, besides the P=N double bond the unsaturation can take a nitrene form, RR′P—N̈:, or a phosphinidene form, RR′N—P̈:. It is known that with only first-row atoms multiple bonding is always preferred over nitrene-like or carbene-like forms;[9] indeed the thermodynamic stability of aminonitrene, H_2N-N, is predicted to be 25 kcal/mol less than that of *trans*-diimide, HN=NH, according to the most refined calculations.[10] When a phosphorus atom is involved, the three forms >P—N, –P=N–, and P—N< compete; their thermodynamic stabilities are not a priori easily predictable. Moreover, a question arises concerning the spin multiplicity (singlet or triplet) of the ground state for the corresponding nitrene or phosphinidene forms.

In this paper, we present an ab initio study of the structures and stabilities of all the H_2PN isomers in their low-lying singlet and triplet states. The three corresponding isomers are therefore

Chart I

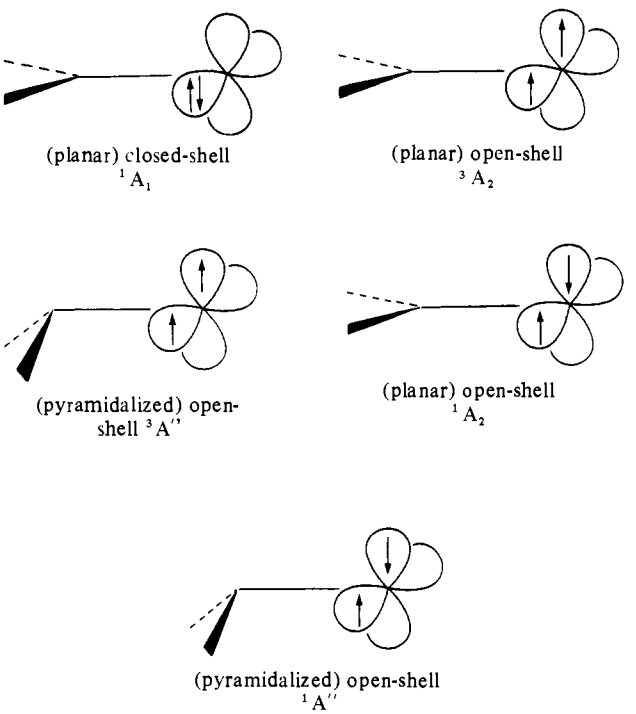

(1) HP=NH (cis and trans), which we shall call phosphazene (phospha(III)azene); (2) H_2P—N̈:, which we shall call phosphinonitrene, without taking into account the hypervalency of phosphorus, but which can be designated as a model for phosphonitriles, $H_2P{\equiv}N$; (3) H_2N—P̈:, which we shall call aminophosphinidene. Emphasis will be put on HP=NH, which is a model for the –P=N– double bond. For our nitrene or phos-

(1) Fluck, E. *Top. Phosphorus Chem.* **1980**, *10*, 193.
(2) N'Gando M'Pondo, T. Thesis, Université Paul Sabatier, Toulouse, France, 1981.
(3) Scherer, O. J.; Kuhn, N.; Jungmann, H. *Z. Naturforsch., B: Anorg. Chem., Org. Chem.* **1978**, *33B*, 1321.
(4) Niecke, E.; Kröher, R. *Z. Naturforsch., B: Anorg. Chem., Org. Chem.* **1979**, *34B*, 387.
(5) Cowley, A. H.; Kilduff, J. E.; Wilburn, J. C. *J. Am. Chem. Soc.* **1981**, *103*, 1575.
(6) Pohl, S. *Angew. Chem., Int. Ed. Engl.* **1976**, *15*, 687.
(7) Pohl, S. *Chem. Ber.* **1979**, *112*, 3159.
(8) Legros, J. P.; Charbonnel, Y.; Barrans, J. *C. R. Hebd. Seances Acad. Sci., Ser. C* **1980**, *291*, 271.
(9) Trinquier, G. Thesis, Université Paul Sabatier, Toulouse, France, 1981 (No. 990).
(10) Parsons, C. A.; Dykstra, C. E. *J. Chem. Phys.* **1979**, *71*, 3025.

0002-7863/82/1504-6969$01.25/0